JACS
JOURNAL OF THE AMERICAN CHEMICAL SOCIETY

ARTICLE

pubs.acs.org/JACS

Rates of Intra- and Intermolecular Electron Transfers in Hydrogenase Deduced from Steady-State Activity Measurements

Sébastien Dementin, Bénédicte Burlat, Vincent Fourmond, Fanny Leroux, Pierre-Pol Liebgott, Abbas Abou Hamdan, Christophe Léger, Marc Rousset, Bruno Guigliarelli, and Patrick Bertrand*

Laboratoire de Bioénergétique et Ingénierie des Protéines, CNRS UPR 9036, 31 chemin Joseph Aiguier, 13402 Marseille Cedex 20, France

Supporting Information

ABSTRACT: Electrons are transferred over long distances along chains of FeS clusters in hydrogenases, mitochondrial complexes, and many other respiratory enzymes. It is usually presumed that electron transfer is fast in these systems, despite the fact that there has been no direct measurement of rates of FeS-to-FeS electron transfer in any respiratory enzyme. In this context, we propose and apply to NiFe hydrogenase an original strategy that consists of quantitatively interpreting the variations of steady-state activity that result from changing the nature of the FeS clusters which connect the active site to the redox partner, and/or the nature of the redox partner. Rates of intra- and intermolecular electron transfer are deduced from such large data sets. The mutation-induced variations of electron transfer rates cannot be explained by changes in intercenter distances and reduction potentials. This establishes that FeS-to-FeS rate constants are extremely sensitive to the nature and coordination of the centers.

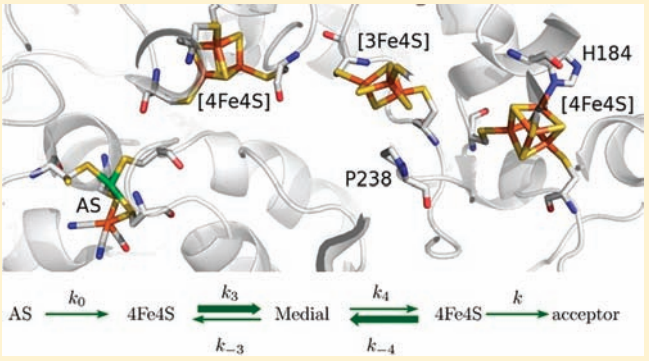

INTRODUCTION

Understanding the mechanisms of energy conversion in living organisms, sometimes with the aim of designing new catalysts for biotechnological transformations, has motivated intensive studies on numerous redox enzymes. Oxidoreductases are often large and structurally complex catalysts whose catalytic cycle comprises steps of very different natures: transport of the substrate and product to and from the active site, active site chemistry, proton transfers, and electron exchanges with the physiological partner via intra- and intermolecular electron transfers. The ability of an enzyme to catalyze a certain reaction is most easily quantified by the Michaelis parameters obtained by fitting the dependence of steady-state turnover rate on reactant concentration. These "global" parameters usually tell us very little about the mechanism and the rates of particular steps in the catalytic cycle, like intramolecular electron and proton transfers, unless it is clearly established that one particular step fully limits turnover. To specifically learn about individual steps, the usual method consists of triggering the cycle and monitoring the evolution of the concentration of reaction intermediates by appropriate spectroscopic techniques.[1] Regarding electron transfer, this approach is well suited for studying photosynthetic reaction centers, whose cycle can be triggered by a flash and whose cofactors are characterized by a large and strongly redox-dependent UV−visible absorbance,[2] but it is much more difficult to implement in the case of respiratory enzymes. Stopped-flow or relaxation experiments can be carried out when the enzyme contains hemes,[3,4] but in many respiratory enzymes like mitochondrial complexes I and II, for example, and certain nitrate reductases or hydrogenases, the cofactors are iron sulfur centers, and the only conceivable fast kinetic technique is freeze-quench coupled to low temperature EPR.[5] Unfortunately, this method is often impracticable because the individual EPR signatures of the centers are blurred by intercenter magnetic interactions.

Another general approach, which we will use in this work, consists of examining how the steady-state kinetic parameters are altered when the substrate or the enzyme is modified. For example, the substrate can be partly or fully deuterated to study kinetic isotope effects. The ability of certain enzymes to catalyze different reactions can also be exploited. This happens, for example, in the case of hydrogenases, which catalyze the oxidation of H_2 and D_2 and the two reverse reactions, as well as the D_2/H^+ and H_2/D^+ exchange reactions.[6] By comparing the activity of a given enzyme in the six reactions, it was possible to identify the rate-limiting steps.[7] Site directed mutagenesis can also be used to specifically alter the rates of certain steps in the catalytic cycle; examining how this affects steady-state turnover may inform on the nature of the rate-limiting step. Hereafter, we shall demonstrate that these experiments can also give information on rate constants.

Received: March 23, 2011
Published: May 26, 2011

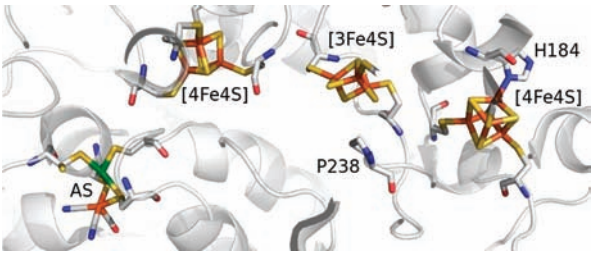

Figure 1. The electron transfer chain that connects the active site (AS) to the protein surface of the NiFe hydrogenase consists of a proximal 4Fe−4S cluster, a medial 3Fe−4S cluster, and a distal 4Fe−4S cluster. The P238C mutation results in 3Fe to 4Fe conversion.[10] The Histidine that ligates the distal cluster can be replaced with Gly (no cluster conversion occurs) or Cys.[16]

In redox enzymes, the electrons involved in the oxidation or the reduction of the substrate are exchanged with the physiological partner via a chain of redox centers that is clearly apparent in X-ray crystal structures. In many cases, the values of the redox potentials determined by potentiometry do not vary in a monotonic fashion along the chain and therefore do not seem to favor efficient and unidirectional transfer. Slow ET may provide an advantage by tuning the "apparent" reduction potential of the active site,[8] but it is most often claimed that even in "thermodynamically unfavorable" conditions, fast transfer is ensured when the intercenter distance is smaller than about 14 Å.[9]

The paradigm of these "anomalous" electron transfer chains is probably that found in many NiFe hydrogenases, where a high potential $[3Fe-4S]^{1+,0}$ cluster is flanked by two $[4Fe-4S]^{2+,1+}$ clusters whose potentials are more negative by about 400 mV (Figure 1). In the enzyme from *Desulfovibrio fructosovorans* (*Df*), converting this high-potential 3Fe−4S cluster into a 4Fe−4S cluster by replacing Pro 238 with a Cys residue shifts 300 mV down the potential of the medial cluster. However, this has only small effects on the H_2 production and oxidation turnover rates, which indicates that intramolecular electron transfer is indeed fast in the native enzyme.[10] Here, we experimentally address the question of how fast electron transfer actually is.

Another particularity of the electron transfer chain of NiFe hydrogenases concerns the ligation of the distal 4Fe−4S cluster, which is exposed to the solvent and is the site of interaction with the physiological partner.[11,12] This cluster is attached to the protein by three cysteine and one histidine residues, instead of four cysteines. This unusual coordination is also found in clostridial FeFe hydrogenases,[13] which are not phylogenetically related to NiFe hydrogenases, in some molybdoenzymes of the DMSO family,[14] and in mitochondrial complex I.[15] When this histidine (His 184) was changed into Gly or Cys in the *Df* enzyme, the redox potential of the distal cluster was not significantly modified, but a strong decrease of the activity of H_2 oxidation by methyl viologen was observed.[16] For example, the cysteine variant has 1% of the activity of the native enzyme. In the case of the glycine mutant, the activity was largely recovered when imidazole was added to the solution, whereas small thiols were found to decrease the turnover rate, presumably because exogenous imidazole and thiols bind to the vacant position of the distal cluster of the glycine variant, thus mimicking the coordination in the native enzyme and the H184C mutant, respectively.[16] These experiments revealed that the efficiency of the electron transfer chain is not determined only by intercenter distances and redox potentials.

All of these experiments provide global, qualitative information on the redox chain. To identify more precisely the factors that determine the kinetics, it is necessary to learn about the rate constants that characterize individual electron transfer steps. We have already mentioned that obtaining information on electron transfers involving FeS centers is not an easy task. This is especially true in the case of NiFe hydrogenases where the proximal and distal 4Fe−4S can be distinguished neither by UV−visible spectroscopy nor by EPR due to intercenter interactions.[17,18] Therefore, this information must be extracted from the only available kinetic data, steady-state activities. In this Article, we show that this can be done by using a realistic kinetic model to analyze a large and consistent data set consisting of the turnover rates measured with six forms of *Df* hydrogenase (wild type, three simple mutants, and two double mutants) and two acceptors (the physiological partner cytochrome c_3 and a redox dye, methyl viologen). The information obtained on intra- and intermolecular electron transfers rates reveals that factors related to details of the protein and to the electronic structure of the FeS clusters play an important role in the efficiency of the chain, in keeping with recent calculations of electron transfer rates in complex I.[19]

MATERIALS AND METHODS

Construction and Purification of the Mutants and of Cytochrome c_3. The *Df* hydrogenase mutants were constructed using the same bacterial strains, plasmids, growth conditions, site-directed mutagenesis strategy, and enzyme purification protocol as described in Leroux et al.[20] The purification yield of the recombinant mutants, abound 1 mg per liter of culture, is similar to that of the WT enzyme, except for H184G, which the bacterium produces in very small amounts.[16]

Although the sequence of the gene coding for the cytochrome c_3 (cyt c_3), which interacts with the *Df* NiFe hydrogenase, is presently unknown, the protein sequence of two putative cyt c_3 can be deduced from the recently released draft of the *Df* genome (Refseq: NZ_AECZ00000000). A detailed study of the complex between the cyt c_3 and the NiFe hydrogenase from *Desulfovibrio vulgaris* Miyazaki F (*Dv*MF) has shown that several acidic residues at the surface of the enzyme interact with lysyl residues of cyt c_3.[11] These acidic residues are conserved in *Df* hydrogenase, and most of the lysyl residues involved in the interaction are conserved (in the strict or contiguous position) in the protein sequence of the putative cyt c_3. Therefore, we used the *Dv*MF cyt c_3 as the "physiological" partner of *Df* hydrogenase. We produced it in a *Shewanella oneidensis* MR-1 strain harboring the plasmid pKFC3 as described by Ozawa et al.[21,22] The purification procedure was as follows. Cells from an overnight 2 L culture (30 °C in LB medium) were harvested by centrifugation, resuspended in Tris/HCl 20 mM pH 7.6 containing 2 mM EDTA (buffer A), and disrupted in a French press. After ultracentrifugation at 30 000*g* for 30 min, the supernatant was dialyzed twice against buffer A and loaded onto a carboxymethyl cellulose CM52 (Whatman) column (6 × 2.5 cm) equilibrated with buffer A. After three 30 mL washings with buffer A containing 0, 50, and 100 mM NaCl, respectively, cyt c_3 was eluted with buffer A containing 250 mM NaCl. No cyt c_3 is adsorbed onto the resin with the supernatant from a *S. oneidensis* strain that does not harbor pKFC3. The eluate was dialyzed twice against buffer A and loaded onto a hydroxyapatite (Biorad) column (6 × 2.5 cm) equilibrated with buffer A. After three 30 mL washings with buffer A containing 0, 50, and 100 mM K_2HPO_3, respectively, cyt c_3 was eluted with buffer A containing 250 mM

K_2HPO_3. The buffer was exchanged against buffer A using Millipore concentrators (Amicon Ultra-15 3000 MWCO). The absorption spectrum of the dithionite reduced sample was typical of that of properly folded cyt c_3.[21,23] The concentration was determined using the absorption coefficient at 552 nm (ε = 115 000 M^{-1} cm^{-1}) of the native protein.[24]

EPR Spectroscopy and Redox Titration. EPR spectra were recorded on a Bruker ELEXSYS E500 X-band spectrometer fitted with an Oxford Instrument ESR 900 helium flow cryostat. The Ni−C signals of the WT, P238C/H184C, and P238C/H184G forms were obtained by adding small amounts (up to 10−20 μL) of a concentrated dithionite solution directly in the EPR tube. The freshly prepared $Na_2S_2O_4$ solution was 100 mM in a 50 mM degassed Hepes buffer (pH8). The FeS centers' EPR signals were obtained by performing redox titrations in the case of the WT, P238C (ref 10), and P238C/H184G forms (see below) and by fully reducing a sample with dithionite in the case of the P238C/H184C variant.

The redox titration of the P238C/H184G mutant was carried out at 25 °C in an anaerobic cell containing a solution of purified enzyme (40 μM) in 50 mM Hepes pH 8 buffer under an argon atmosphere. Redox potentials were measured with a combined Pt−Ag/AgCl/KCl (3 M) microelectrode, in the presence of the following mediators (5 μM each): resorufine, indigo carmine, phenosafranine, neutral red, and methyl viologen. The titration was conducted by stepwise additions of small amounts of sodium dithionite solution (20 mM in oxygen-free Hepes buffer). At each equilibrium, 150 μL of the solution was transferred anaerobically into calibrated EPR tubes, which were rapidly frozen, and the spectra were recorded at 6 K. All potentials are quoted against the standard hydrogen electrode.

H_2 Oxidation Assay. Activity measurements were performed using the same protocol for the six forms of the enzyme. The Michaelis constants for H_2 of the P238C, H184C, and H184G mutants (the latter in the absence or in the presence of 10 mM imidazole) were determined at pH 7, 40 °C, by using protein film voltammetry (PFV),[25] as described previously.[26] The Michaelis constants of the WT and all of these variants of the enzyme are small, in the range 5−15 matm H_2. The solution assays were carried out under 1 atm of H_2 (that is, under saturating conditions).

The H_2 oxidation activity was measured with two acceptors, a redox dye, methyl viologen (MV, $E°$ = −450 mV at pH 7), and *Dv*MF cytc_3, which contains four hemes whose redox potentials are in the range from −250 to −360 mV at pH 8.[27] The purified enzymes were activated, and the kinetic parameters with MV were determined at 30 °C, pH8, as described in refs 16,20. For the activity measurements with cyt c_3, the WT and mutated enzymes were activated 1 h at 37 °C in an anaerobic cuvette containing H_2-bubbled Tris/HCl 0.1 M, MV 0.2 mM in the presence of glucose oxidase (10 u), catalase (200 u), and glucose (10 mM) to scavenge O_2. The cyt c_3 reduction activity was determined at 30 °C in a UV cuvette containing 1 mL of Hepes 50 mM pH 7.5 flushed with H_2 for 10 min. The concentration of cyt c_3 was in the range 1−7 μM. The cuvette was incubated for 10 min at 30 °C before 5−20 μL of activated enzyme was added to start the reaction. The reduction of cyt c_3 was measured at 552 nm with a UV 1601 spectrophotometer (Shimadzu). The slope at the beginning of timedrive was used to calculate the activity using the absorption coefficient of 84 000 M^{-1} cm^{-1} as described in ref 11. The parameters K_m and k_{cat} were determined by fitting the data to the Michaelis−Menten equation. In the following, all k_{cat} values are expressed in units of electrons s^{-1}, noting that the full absorbance variation between oxidized and reduced cyt c_3 requires 4 electrons.

KINETIC MODEL

To analyze the changes in k_{cat} values that occur when the electron transfer chain is modified, we use a kinetic model in

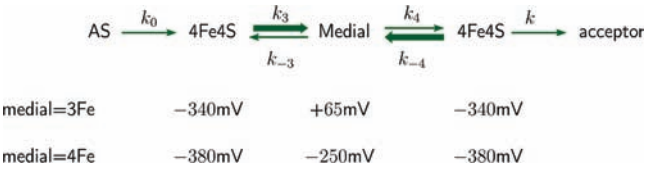

Figure 2. Definition of the rate constants used in the kinetic model. The "thermodynamically favored" rate constants are shown with bold arrows. The reduction potentials of the clusters are indicated depending on whether the medial cluster is a 3Fe−4S or a 4Fe−4S cluster.

which the reversible exchanges between the redox centers are explicitly considered and the electron flux generated by the oxidation of H_2 is described by an effective first-order rate constant k_0 (Figure 2). Some peculiarities of the experimental conditions have to be taken into account. The k_{cat} values are obtained with saturating concentrations of the electron acceptors and of H_2, so that rates are zero-order in substrates. Besides, because we consider initial rates, the rate of backward intermolecular transfer remains small and was neglected (Figure 2). The chain can exist in 2^3 = 8 states defined by a certain combination of redox states of the FeS centers, and the possible transitions between these 8 states are defined in the kinetic scheme of Figure 3. The steady-state populations are expressed in terms of rate constants by standard methods (Supporting Information, section 1), and the first-order rate of reduction of the acceptor, k_{cat}, equates k times the total population of states in which the distal center is reduced. Because four states, whose populations are noted x_2, x_5, x_6, x_8 in Figure 3, contribute to the reduction of the acceptor, the general expression of k_{cat} is very complicated, a fact that has been overlooked before. In the particular case of NiFe hydrogenases, it can be simplified because the medial cluster has much greater reduction potential than the side clusters, and therefore the equilibrium constants:

$$K_3 = k_3/k_{-3},\ K_{-4} = k_{-4}/k_4 \qquad (1)$$

are much larger than unity. Indeed, these equilibrium constants, which are given by

$$K_3 = \exp(F(E_m^0 - E_p^0)/RT),$$
$$K_{-4} = \exp(F(E_m^0 - E_d^0)/RT)$$

where E_p^0, E_m^0, and E_d^0 are the potentials of the proximal, medial, and distal centers, are equal to about 10^7 when the medial cluster is a 3Fe−4S cluster (E_m^0 = +65 mV, $E_p^0 = E_d^0$ = −340 mV) and about 200 when it is a 4Fe−4S (E_m^0 = −250 mV, $E_p^0 = E_d^0$ = −380 mV).[10] With $K_{-4} \gg 1$ and $K_3 \gg 1$, k_{cat} is given by eq S14 in Supporting Information section 1. A simplified expression is obtained by assuming $k_0K_{-4}/k \gg 1$ and $k_3 \gg k$. The consistency of these hypotheses will be checked a posteriori. Under these conditions, one obtains (Supporting Information section 1):

$$\frac{1}{k_{cat}} = \frac{1}{k_0} + \frac{K_{-4}}{k_3} + \frac{1}{k_4} + \frac{1}{k} + \frac{(K_{-4}/K_3) - 1}{k + k_0} \qquad (2)$$

This expression, which reflects the intrinsic complexity of the kinetic scheme (Figure 3), contrasts with the simple sum of the reciprocal of the forward rate constants, which would be obtained if all steps were irreversible ($1/k_{cat} = 1/k_0 + 1/k_3 + 1/k_4 + 1/k$). The interpretation of some terms of eq 2 is not at all intuitive. In the second term of the right-hand side of eq 2, the reciprocal of k_3, which corresponds to a presumably fast transfer toward the medial cluster (Figure 2), is weighted by the large equilibrium

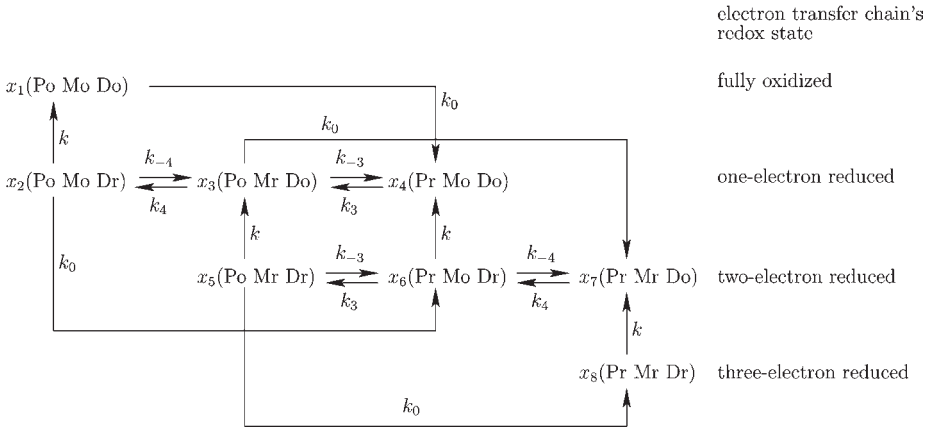

Figure 3. Kinetic scheme connecting the eight redox states of the electron transfer chain of NiFe hydrogenases that can exist during turnover. The "P", "M", and "D" letters refer to the proximal, medial, and distal clusters, and the subscripts "o" or "r" indicate their redox state.

constant K_{-4}. The rightmost term of eq 2, which has an unusual form, shows the influence of the asymmetry of the chain, measured by the ratio K_{-4}/K_3. This ratio is determined by the difference between the redox potentials of the proximal and distal 4Fe−4S clusters:

$$K_{-4}/K_3 = \exp(F(E_p^0 - E_d^0)/RT)$$

According to eq 2, decreasing the difference $(E_p^0 - E_d^0)$ increases k_{cat}, as expected. We shall see in the next section that the redox potentials of the proximal and distal clusters are essentially insensitive to the mutations and that their difference is small in *Df* hydrogenase. Therefore, we will analyze the data in the framework of a fully symmetric $(K_{-4} = K_3)$ electron transfer chain. This makes it possible to write eq 2 in a convenient form that does not introduce any significant bias in the analysis of the results. We obtain:

$$1/k_{cat} = 1/k_0 + 1/k_{-3} + 1/k_4 + 1/k \quad (3)$$

We have used $K_3/k_3 = k_{-3}$ (eq 1). This simple expression involves only the "smallest" rate constants defined in Figure 2, including k_{-3}, which characterizes a backward electron transfer. It is useful to combine the first three terms and define:

$$1/k_i = 1/k_0 + 1/k_{-3} + 1/k_4 \quad (4)$$

so that eq 3 now reads:

$$1/k_{cat} = 1/k_i + 1/k \quad (5)$$

This form is practical to analyze the data because $1/k_{cat}$ appears as the sum of two terms, which react differently to modifications of the electron transfer chain (Figure 2):

- k_i is an effective rate constant, which depends on all intramolecular steps (eq 4): k_0 accounts for the diffusion of H_2 to the active site, the chemistry at the active site, and electron transfer to the proximal 4Fe−4S cluster, and it is expected to be weakly sensitive to modifications of the redox chain. In contrast, k_{-3} and k_4 depend on the nature (3Fe−4S or 4Fe−4S) of the medial center, and k_4 is also dependent on the coordination of the distal 4Fe−4S cluster.
- k is the intermolecular rate constant, which depends on the coordination of the distal cluster and on the nature of the acceptor.

Thus, although measuring a single value of k_{cat} does not suffice to determine k_i and k, quantitative information about the two contributions can be obtained by analyzing the changes of k_{cat}, which result from the conversion of the 3Fe−4S (this modifies k_i) and/or the change of acceptor (this modifies k). This is the strategy we use hereafter.

RESULTS

1. EPR Spectra and Redox Titration. The EPR spectra of the P238C/H184C and P238C/H184G mutants were recorded at different temperatures and in various redox states to analyze the structural changes of the metal centers. The high temperature spectra, which reflect the structure of the NiFe active site, are very similar to those given by the WT enzyme. In the oxidized state, the spectrum comprises a major Ni−A (g = 2.32, 2.23, 2.01) and a minor Ni−B (g = 2.34, 2.16, 2.01) component due to inactive forms of the enzyme (Figure 4A). In the reduced state, the Ni−C signal (g = 2.19, 2.14, 2.01) due to an intermediate in the catalytic cycle was observed (Figure 4B).

The low temperature spectra report on the nature and the structure of the FeS clusters. As expected, the spectra of the double mutants differ from those of the native form. In the oxidized state, the WT enzyme displays the spectrum of the $[3Fe-4S]^{1+}$ cluster (Figure 4C, spectrum a). Upon reduction, this signal disappears and is replaced by a large and dissymmetric signal at low field, typical of a reduced $[3Fe-4S]^0$ cluster with a S = 2 ground state (data not shown). At very low potential, the two 4Fe−4S clusters become reduced (and paramagnetic), and a broad spectrum due to the interactions with the $[3Fe-4S]^0$ cluster appears (Figure 4D, spectrum f). In contrast, the double mutants are EPR silent in the oxidized state (Figure 4C, spectra b,c). Upon reduction, the P238C/H184G variant gave an EPR signal typical of a $[4Fe-4S]^{1+}$ cluster (Figure 4D, spectrum b), which changed into a broad signal at very low potential (Figure 4D, spectrum d). All of these signals are identical to those observed in the case of the P238C mutant (Figure 4D, spectra a,c). In particular, the shape of the broad signal, which results from the interactions between three $[4Fe-4S]^{1+}$ clusters with S = 1/2, differs significantly from that given by the WT form, which results from the interactions between one $[3Fe-4S]^0$ (S = 2) and two $[4Fe-4S]^{1+}$ clusters (Figure 4D, spectrum f). Although no detailed redox titration was carried out with the P238C/H184C variant,

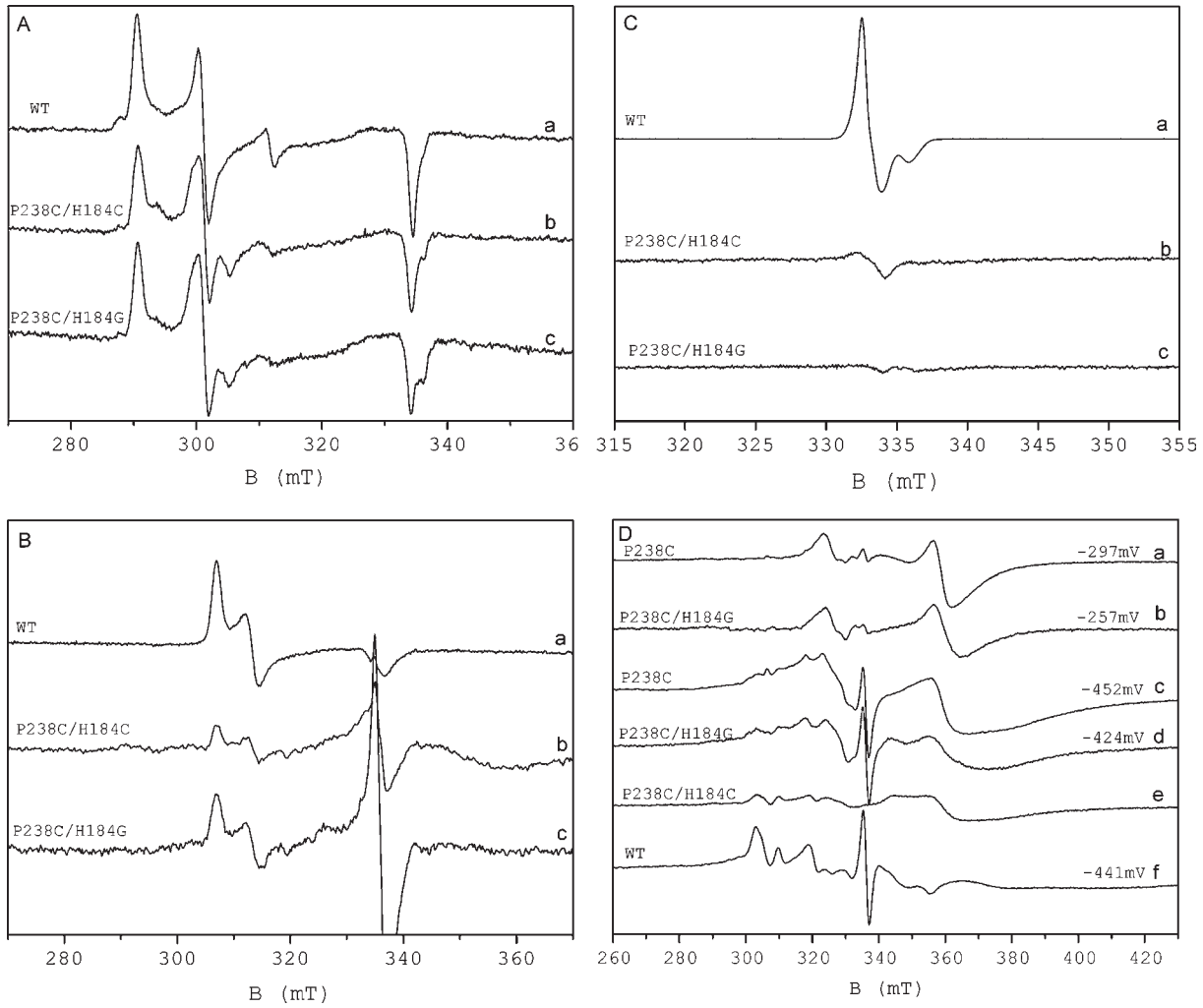

Figure 4. EPR spectra of oxidized and reduced WT and mutant NiFe hydrogenases. (A,C) As-prepared enzymes. Experimental conditions: temperature (T), (A) 100 K, (C) 15 K; modulation amplitude (MA), (A) 1 mT, (C) 0.5 mT; microwave power (P), (A) 10 mW, (C) WT 0.4 mW, mutants 1 mW. Microwave frequency (ν): (A) 9.4064 GHz, C) 9.4069 GHz. (B) Ni−C signals. T = 30 K; MA = 1 mT; P = 10 mW; ν = 9.4065 GHz. (D) Signals displayed by the FeS centers during a potentiometric titration. T = 6 K; MA = 1 mT; microwave power (a,b,d) 1 mW, (c) 4 mW, (e,f) 10 mW. ν = 9.4078 GHz. The enzyme concentration was 40 μM (A−C) and 100 μM (D) for the WT form, 20 μM (A−D) for P238C/H184C, 20 μM (A−C) and 40 μM (D) for P238C/H184G, and 100 μM for P238C (D).

we have checked that the interaction spectrum displayed by a fully reduced sample of this form was identical to that given by the P238C and P238C/H184G mutants (Figure 4D, spectrum e).

This study shows that, in the double mutants, the 3Fe−4S cluster was converted into a medial 4Fe−4S cluster whose EPR spectrum is identical to that observed for the P238C form.[10] These experiments and the $K_m(H_2)$ measurements also demonstrate that the structure of the active site is not altered by the mutations. Thus, the steps of the catalytic cycle that determine the magnitude of the electron flux supplied to the redox chain (diffusion of H_2 to the active site, chemistry at the active site, and electron transfer from the active site to the proximal cluster), are expected to be unchanged by these mutations. Accordingly, one can consider that the effective rate constant k_0, which appears in the kinetic model (Figure 2), has the same value in the six forms of the enzyme studied in this work (but note that our results would not be affected if the values of k_0 were not exactly the same in all variants).

To examine the effects of a double mutation on the potentials of the FeS clusters, a detailed redox titration monitored by EPR was carried out with the P238C/H184G form, and the results were interpreted by using the formalism that was applied before to the P238C mutant,[10] which is described in Supporting Information section 2. The variation of the EPR spectrum as a function of the electrode potential shows that the medial 4Fe−4S cluster is reduced before the broadening due to the interactions with the two other 4Fe−4S clusters appears (Supporting Information Figure S2). As a result, the titration can be analyzed by using five redox states and three redox potentials: E_m^0, the potential of the medial cluster when the proximal and distal clusters are oxidized, and E_p^0, E_d^0, the potentials of the proximal and distal centers when the medial cluster is reduced (Supporting Information Figure S3). The expressions of the five populations as a function of E_m^0, E_p^0, E_d^0, and the electrode potential E were used to fit the variation of characteristic features of the spectrum and of its full intensity. The best fits were obtained with $E_m^0 = -270 \pm 20$ mV, $E_p^0 = -380 \pm 20$ mV, and $E_d^0 = -380 \pm 20$ mV (Supporting Information Figure S4). These values are essentially identical to those obtained with the P238C form of the enzyme ($E_m^0 = -250$ mV, $E_p^0 = E_d^0 = -380$ mV),[10] which confirms that

dx.doi.org/10.1021/ja202615a |J. Am. Chem. Soc. 2011, 133, 10211–10221

Table 1. Steady-State Turnover Rates of H_2 Oxidation Obtained with the Six Variants of *D. fructosovorans* NiFe Hydrogenase and Two Redox Acceptors, in Units of electrons s^{-1}[a]

redox partner	MV	c_3	MV	c_3	MV	c_3
exogenous ligand	none	none	0.1 M imidazole	14 mM imidazole	14 mM mercaptoethanol	3 mM mercaptoethanol
WT	1500 (a)	1050 (g)	(m)		(m)	
P238C	390 (b)	370 (h)				
H184G	45 (c)	90 (i)	450	570	5	6
P238C/H184G	360 (d)	66 (j)	540	180	260	40
H184C	25 (e)	1.5 (k)	(m)		(m)	
P238C/H184C	480 (f)	40 (l)				

[a] k_{cat} values were deduced from activity measurements carried out with 0.5−500 mM methyl viologen (MV), and 1−7 μM cytochrome c_3. Experimental conditions: 30 °C, pH 8 (MV) and pH 7.5 (cyt c_3), 1 atm H_2. The values of K_m(MV) are (a) 9 mM, (b) 3.8 mM, (c) 2.2 mM, (d) 2.2 mM, (e) 16 mM, (f) 2.1 mM. The K_m (cytochrome c_3) values are (g) 1.5 μM, (h) 2.8 μM, (i) 0.4 μM, (j) 0.7 μM, (k) <2 μM, (l) 1.5 μM. (m) Imidazole and mercaptoethanol have no effect on the activity of the WT and H184C enzymes (see ref 16).

changing the coordination at the distal 4Fe−4S cluster (P238C to P238C/H184G) does not appreciably alter the potential of the cluster.[16] In the following, the kinetic data are analyzed by using the values reported in ref 10.

2. Steady-State Activity Measurements. The Michaelis parameters measured for H_2 oxidation with the six forms of *Df* hydrogenase and the two acceptors are reported in Table 1. The K_m(MV) and $K_m(c_3)$ are in the range 2−15 mM and 0.5−3 μM, respectively. The apparent affinity for the acceptors of the H184G, P238C/H184G, and P238C/H184C variants is equal to or greater than that of the WT form, which demonstrates that the position 184 residue is not a molecular determinant of the enzyme-partner recognition, consistent with the demonstration that the formation of the complex between hydrogenase and cytochrome c_3 is governed by electrostatic interactions between acidic and basic surface residues.[11] The accuracy of the turnover rate values ranges from ±10% to ±20%, depending on the form of the enzyme. The activity is maximum for the WT form, and it varies largely in the series, from 1500 to 25 s^{-1} with MV and from 1050 to 1.5 s^{-1} with cyt c_3. Thus, the thermodynamic driving force provided by the oxidation of H_2 by the acceptors is used very differently by the six forms of the enzyme, and the results of the EPR experiments indicate that these differences come from the modifications of the electron transfer chain. In the case of the H184G variant, the spectacular rescue by exogenous imidazole and the inhibition by mercaptoethanol, which were discovered by using MV or an electrode as acceptor,[16] are also observed with cyt c_3. The same effects occur with the P238C/H184G form, but to a lesser extent, especially when MV is the acceptor.

Converting the medial center into a 4Fe−4S cluster is expected to affect essentially intramolecular electron transfers, whereas modifications of the distal center can alter both intra- and intermolecular steps. Thus, it is simpler to analyze the data by comparing the activities of forms of the enzyme that differ only by the nature of the medial center.

We introduce the following notations (Figure 5):

- The intermolecular rate constant k and the turnover number k_{cat} are indexed with 1 and 2 when the acceptors are MV and cyt c_3, respectively.
- The turnover numbers and the rate constants are unlabeled when the medial center is a 3Fe−4S cluster and labeled with a prime when it is a 4Fe−4S cluster.

Applying eq 5 to the four reactions of Figure 5 gives:

$$1/k_{cat1} = 1/k_i + 1/k_1;\ 1/k_{cat1}' = 1/k_i' + 1/k_1'$$

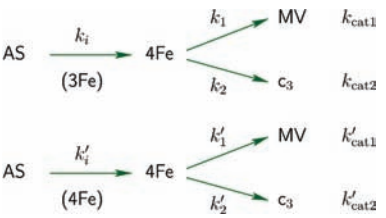

Figure 5. Notations used in the analysis of the k_{cat} values reported in Table 1. The intermolecular rate constant k and the turnover number k_{cat} are indexed with 1 and 2 when the acceptors are MV and cytochrome c_3, respectively. The turnover numbers and the rate constants are unlabeled when the medial center is a 3Fe−4S cluster and labeled with a prime when it is a 4Fe−4S cluster.

$$1/k_{cat2} = 1/k_i + 1/k_2;\ 1/k_{cat2}' = 1/k_i' + 1/k_2'$$

From these equations, we deduce:

$$1/k_{cat1}' - 1/k_{cat1} = (1/k_i' - 1/k_i) + (1/k_1' - 1/k_1)$$

$$1/k_{cat2}' - 1/k_{cat2} = (1/k_i' - 1/k_i) + (1/k_2' - 1/k_2)$$

The conversion of the medial center is not expected to affect intermolecular transfers ($k_1 = k_1'$, $k_2 = k_2'$). Therefore, the experimental data should verify:

$$1/k_{cat1}' - 1/k_{cat1} = 1/k_{cat2}' - 1/k_{cat2} = 1/k_i' - 1/k_i \quad (6)$$

Comparison of the Wild Type and P238C Forms. From the data reported in Table 1, we deduce $(1/k_{cat1}' - 1/k_{cat1}) = 1.9 \times 10^{-3}$ s and $(1/k_{cat2}' - 1/k_{cat2}) = 1.75 \times 10^{-3}$ s. Equation 6 is obeyed to within 10%, which is better than the accuracy of the measurements. Thus, the assumption $k_1 = k_1'$, $k_2 = k_2'$ is correct. We continue the analysis by noting that eq 5 implies:

$$k_i > k_{cat},\ k > k_{cat} \quad (7)$$

Applying these inequalities to the data gives (Figure 6a):

$$k_i > 1500\ s^{-1},\ k_i' > 390\ s^{-1},\ k_1 > 1500\ s^{-1},$$
$$k_2 > 1050\ s^{-1},\ \text{with } k_1 > k_2 \quad (8)$$

An upper limit for k_2 can be deduced from $1/k_2 = 1/k_{cat2} - 1/k_i$. Using $k_i > 1500\ s^{-1}$ (eq 8), we deduce:

$$k_2 < 3500\ s^{-1} \quad (9)$$

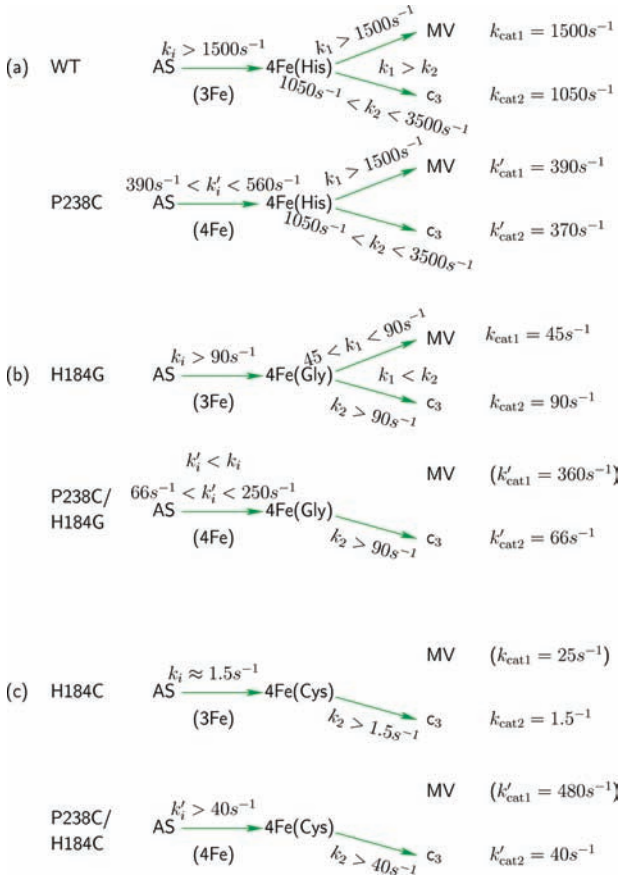

Figure 6. Values of the intra- and intermolecular rate constants (defined in eq 5 and Figure 5) in the six hydrogenase variants, determined by analyzing the steady-state turnover rates.

Together with eq 8, this gives an interval for k_2. To get more information about the intramolecular steps, we use eq 6. From $(1/k_{cat2}' - 1/k_{cat2}) = 1.75 \times 10^{-3}$ s, we deduce $1/k_i' = 1/k_i + 1.75 \times 10^{-3}$ s. This implies $k_i' < k_i$. Because $1/k_i$ is positive, this also implies $1/k_i' > 1.75 \times 10^{-3}$ s and therefore:

$$k_i\prime < 560\ \mathrm{s}^{-1} \qquad (10)$$

Using eq 8, we obtain an interval for k_i'. The results are presented in Figure 6a, and they can be summarized as follows: (1) Converting the 3Fe−4S cluster into a 4Fe−4S cluster decreases k_i more than 3-fold ($k_i > 1500\ \mathrm{s}^{-1}$ in WT and $k_i' < 560\ \mathrm{s}^{-1}$ in P238C). (2) In the P238C variant, k_i' is at least twice as small as the intermolecular rate constants k_1 and k_2. (3) The data do not tell us which step is rate limiting in the wild type form. Indeed, they are consistent with either of the following limiting situations: (i) $k_i \gg 1500\ \mathrm{s}^{-1}$, $k_1 = 1500\ \mathrm{s}^{-1}$, $k_2 = 1050\ \mathrm{s}^{-1}$ (this would imply that intermolecular electron transfer fully limits turnover), or (ii) $k_i = 1500\ \mathrm{s}^{-1}$, $k_1 \gg 3500\ \mathrm{s}^{-1}$, $k_2 = 3500\ \mathrm{s}^{-1}$ (in which case the rates of the intramolecular steps and of the intermolecular transfer to cyt c_3 are similar).

Comparison of the H184G and P238C/H184G Forms. From the data reported in Table 1, we deduce $(1/k_{cat1}' - 1/k_{cat1}) = -1.9 \times 10^{-2}$ s and $(1/k_{cat2}' - 1/k_{cat2}) = 4 \times 10^{-3}$ s. The relation (eq 6) is not obeyed, which means that some assumptions made in the model do not apply to these forms. The origin of this discrepancy appears if one considers the changes of activity due to the addition of imidazole or mercaptoethanol: when MV is the acceptor, these changes are much smaller in the P238C/H184G form than in the H184G form (Table 1). The simplest explanation is that electron transfer via the distal center is strongly slowed in the P238C/H184G form of the hydrogenase, so that a direct transfer from the low potential medial 4Fe−4S cluster to an oxidized MV molecule bound somewhere at the surface of the protein becomes more efficient. Such short circuit is not possible with the cytochrome, which is condemned to receive electrons from the distal center.

This phenomenon has methodological implications concerning the use of redox dyes in studies of redox enzymes (see Discussion), and it limits the information that can be deduced here from the turnover numbers measured with these forms of the enzyme. This is because the kinetic scheme used to derive eq 5 does not apply in this case when MV is the acceptor, so that the k_{cat1}' values must be disregarded.

The method used to derive eq 8 leads to:

$$k_i > 90\ \mathrm{s}^{-1},\ k_i\prime > 66\ \mathrm{s}^{-1},\ k_1 > 45\ \mathrm{s}^{-1},\ k_2 > 90\ \mathrm{s}^{-1},\ \text{with}\ k_2 > k_1$$

From $1/k_1 = 1/k_{cat1} - 1/k_i$ and $k_i > 90\ \mathrm{s}^{-1}$, an upper limit for k_1 is obtained:

$$k_1 < 90\ \mathrm{s}^{-1}$$

To get information about intramolecular steps, we use $(1/k_i' - 1/k_i) = (1/k_{cat2}' - 1/k_{cat2}) = 4 \times 10^{-3}$ s (eq 6), which gives:

$$k_i\prime < 250\ \mathrm{s}^{-1},\ k_i\prime < k_i \qquad (11)$$

The results are reported in Figure 6b. We conclude the following. (1) As observed with the WT and P238C forms, the conversion of the medial center decreases k_i when there is a glycine at the 184 position (eq 11), but in this case by an amount that cannot be specified. (2) The comparison of Figure 6a and b shows that substituting Gly for His184 slows strongly the intermolecular transfer to MV when the medial center is a 3Fe−4S cluster ($k_1 > 1500\ \mathrm{s}^{-1}$ in WT as compared to $k_1 < 90\ \mathrm{s}^{-1}$ in H184G) and decreases k_i' by a factor in the range 2−10. (3) When the medial cluster is a 4Fe−4S, a short circuit is suspected.

Comparison of the H184C and P238C/H184C Forms. For these mutants, we calculate $(1/k_{cat1}' - 1/k_{cat1}) = -3.8 \times 10^{-2}$ s and $(1/k_{cat2}' - 1/k_{cat2}) = -6 \times 10^{-1}$ s. The relation (eq 6) is not obeyed, which strongly suggests that a short circuit also occurs in the P238C/H184C form. Therefore, the k_{cat1}' values are disregarded in the analysis. Applying the same treatment as above, we obtain:

$$k_i > 25\ \mathrm{s}^{-1},\ k_i\prime > 40\ \mathrm{s}^{-1},\ k_1 > 25\ \mathrm{s}^{-1},\ k_2 > 40\ \mathrm{s}^{-1},\ \text{with}\ k_1 > k_2 \qquad (12)$$

Using $1/k_2 = 1/k_{cat2} - 1/k_i$ and $k_i > 25\ \mathrm{s}^{-1}$ to obtain an upper limit for k_2, we get $k_2 < 1.6\ \mathrm{s}^{-1}$, which is not consistent with eq 12. The most likely explanation is that electron transfer via the distal center is strongly impaired in the H184C form of the enzyme, so that electrons are directly transferred from the medial 3Fe−4S cluster to a MV molecule bound on the surface. Therefore, we use only the data obtained with cyt c_3:

$$k_i > 1.5\ \mathrm{s}^{-1},\ k_i\prime > 40\ \mathrm{s}^{-1},\ k_2 > 40\ \mathrm{s}^{-1}$$

From $1/k_i = 1/k_{cat2} - 1/k_2$ and $k_2 > 40\ \mathrm{s}^{-1}$, we deduce $k_i \approx 1.5\ \mathrm{s}^{-1}$.

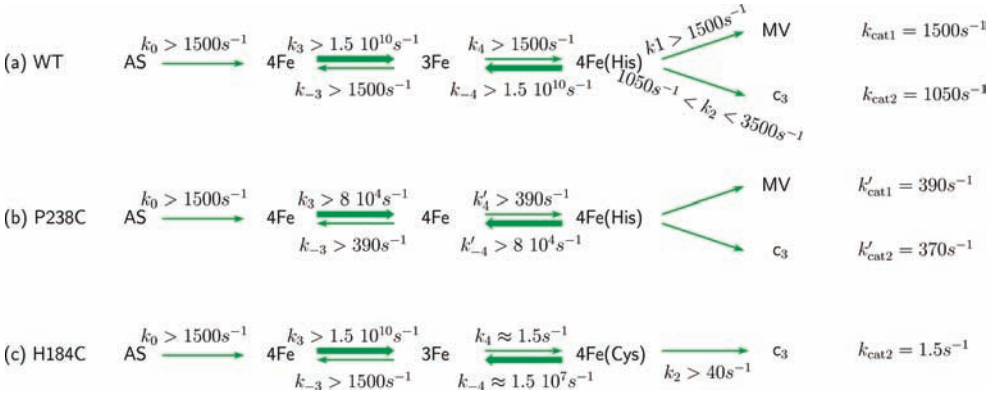

Figure 7. Values of the center-to-center electron transfer rate constants in the six *D. fructosovorans* hydrogenase variants, determined by analyzing the data in Figure 6 with eqs 1 and 4.

The results are presented in Figure 6c. Most remarkably, when the medial center is a 3Fe−4S cluster, k_i is decreased by 3 orders of magnitude when the His residue coordinating the distal center is changed into Cys.

Individual Rate Constants. The next step in our analysis is to deduce the individual rate constants defined in Figure 2 from the values of k_i. Equation 4 shows that k_0, k_{-3}, and k_4 are all larger than k_i. Using the results collected in Figure 6, lower limits for these rate constants can be set for all enzyme forms, and lower limits for k_3 and k_{-4} are then deduced from the experimental equilibrium constants (eq 1). Figure 7 shows the results obtained for the WT and P238C forms, which will be discussed in detail hereafter. We have also shown the results obtained for the H184C form. Because k_0 and k_{-3} are expected to be larger than 1500 s^{-1} as in the native enzyme, we deduce $k_4 = k_i \approx 1.5$ s^{-1}.

The information gained on the rate constants can be used to check the validity of some assumptions used to derive eq 2 (see the Kinetic Model section). First, the ratio k_0K_{-4}/k was assumed to be much larger than unity. Using the upper limit of k_2 and the lower limit of k_0, this quantity is indeed found to be larger than 4×10^6 in the wild type form and larger than 90 in the P238C form. The second assumption, that k_3 and k_3' are both much larger than k_2, is also consistent with the results. This is even truer for the other forms of the enzyme in which k_2 is expected to be smaller (Figure 6).

DISCUSSION

We have devised an original method to get quantitative information about the rate constants of individual electron transfer steps in NiFe hydrogenase. It consists of analyzing in detail a set of steady-state turnover rates determined with various forms of the enzyme in which the redox chain has been modified. The modifications concerned the nature of the medial center (3Fe−4S or 4Fe−4S), the coordination of the distal center by the position 184 residue (His, Gly, Cys), and the nature of the electron acceptor (MV or cyt c_3). Control experiments strongly suggest that these mutations do not alter the steps that occur prior to electron transfer from the active site to the proximal cluster. The steady-state activity changes were analyzed with a kinetic model (Figure 3) that takes into account the reversibility of all electron transfers to establish the rather complex relation between turnover rate and individual electron transfer rates in an enzyme whose redox chain is made of three relays (Supporting Information eq S14). In the case of NiFe hydrogenases, this relation can be greatly simplified because the reduction potential of the medial cluster is much more positive than the other two, and because the redox chain is essentially symmetrical (the proximal and distal centers have similar reduction potentials). The steady-state turnover rate is not obtained by simply summing the reciprocal of the rate constants corresponding to forward electron transfers, but it takes nonetheless a very simple form (eq 3), which can be written as the sum of two terms (eq 5) to separate the contributions of intermolecular electron transfer and intramolecular steps (k and k_i, respectively). We then examined how the turnover rate is affected by changing the medial center (this affects intramolecular ET) and the acceptor (this affects intermolecular ET), to bound the values of the rate constants k and k_i. The results of this analysis are summarized in Figure 6. We shall now interpret the values of these two parameters to learn about the rate constants of the individual steps (our results are summarized in Figure 7) and the factors that determine them.

Intramolecular Electron Transfer. We recall that in the high temperature limit, the rate constant for long distance electron transfer from a donor D to an acceptor A is given by:

$$k_{ET} = \frac{2\pi}{\hbar} \frac{V^2}{\sqrt{4\pi\lambda k_B T}} \exp\left(-\frac{(\Delta G^0 + \lambda)^2}{4\lambda k_B T}\right) \qquad (13)$$

- V^2 is the electronic factor, which is determined by the overlap of the donor and acceptor orbitals. It depends on the nature and orientation of the redox centers, on the intercenter distance, and on the intercenter medium.
- $\Delta G^\circ = -e\Delta E^\circ$ is the standard Gibbs free energy change per molecule, e is the elementary charge, and $\Delta E^\circ = E^\circ(A) - E^\circ(D)$ is the difference between the standard potentials of the acceptor and the donor.
- λ is the reorganization energy. It is the free energy required to change the geometry of the whole system from its equilibrium value when the electron is on the donor to its equilibrium value when the electron is on the acceptor. It can be written as

$$\lambda = \lambda_{in} + \lambda_{out} \qquad (14)$$

where λ_{in} is the inner-sphere contribution due to the different geometry of the oxidized and reduced redox centers and λ_{out} is

the outer-sphere contribution due to the reorganization of the protein and of the solvent. Biological electron transfers usually take place in the "normal" region ($|\Delta G^\circ| < \lambda$), where the rate constant is enhanced when ΔE° increases and λ decreases.

Let us first consider the effects of the conversion of the 3Fe−4S cluster into a 4Fe−4S cluster. When the distal center is coordinated by the side chain of a His residue (H184), this conversion decreases k_i at least 3-fold (Figure 6a). A decrease is also observed when H184 is replaced with Gly (Figure 6b). This is due to the decrease of one or several of the rate constants k_0, k_{-3}, k_4 (eq 4). Because k_0 is not sensitive to modifications of the electron transfer chain, we ascribe the decrease of k_i to that of k_{-3} and/or k_4, noting that both rate constants should depend strongly on the nature of the medial center. Indeed, converting this center into a 4Fe−4S cluster increases ΔE° from −400 to −130 mV, which should strongly increase both rate constants. Therefore, our results show that this favorable effect is more than compensated by unfavorable changes of other parameters, which result in the decrease of k_{cat} that is observed experimentally (Figure 6 and Table 1). To explain this, a first possibility is an increase of the reorganization energy λ when the medial 3Fe−4S cluster is changed into a 4Fe−4S cluster. Assuming that k_{-3} and k_4 are characterized by λ values in the range 0.6−1 eV in the WT form, simple calculations based on eq 13 demonstrate that an increase of λ of about 0.7 eV is needed for compensating the increase of ΔE°. To examine the possibility of such an increase, we searched for data reported in the literature, but experimental and calculated λ values for electron transfers involving FeS clusters are scarce and our quest was vain (see section 3 in the Supporting Information). A clear answer about the possibility of a large increase of λ due to the conversion of the 3Fe−4S to 4Fe−4S cluster would require theoretical calculations based on the structure of the enzyme. However, the fact that this conversion leads to a decrease of k_i when the position 184 amino acid is a histidine or a glycine (Figure 6a and b), and to an increase of k_i when it is a Cys residue (Figure 6c), shows that the rate constants are not determined solely by ΔE° and λ, and that the electronic factor also plays an important role. Putative electron transfer pathways connecting pairs of redox centers were described in the X-ray structure of the *Desulfovibrio gigas* enzyme at 2.85 Å resolution.[28] They are made of covalent bonds, metal−ligand bonds, and NH−S hydrogen bonds. These pathways are well conserved in the structure of the hydrogenase from *D. fructosovorans* (pdb 1YQW, 1.8 Å resolution) and also in that of *D. baculatum* (1CCI, 2.15 Å resolution) in which the medial center is a 4Fe−4S cluster. The only significant difference is the length of the hydrogen bond between Cys 246 (*D. gigas* numbering), a ligand of the medial cluster, and Cys 219, a ligand of the distal center, which is equal to 3.4 Å in *D. fructosovorans* and 3.7 Å in *D. baculatum*. Thus, these putative electron transfer pathways are not expected to be altered by the 3Fe−4S to 4Fe−4S conversion in the *Df* enzyme. However, it should be noted that the electronic factor V^2 (eq 13) depends on the electron tunneling pathway but also on the nature of the redox centers. Calculations like those described in ref 19 would therefore be needed to evaluate the effect of the conversion of the 3Fe−4S cluster into a 4Fe−4S cluster on the electronic factor.

We now consider the effects of coordination changes at the distal 4Fe−4S cluster. The most spectacular result is the more than 3 orders of magnitude decrease of k_4 (ET from medial to distal cluster) when His 184 is replaced by a Cys residue (Figure 7a,c) despite the fact that the reduction potential of the distal cluster is not significantly modified (see Results). This is probably due to a strong increase of the reorganization energy. Indeed, the inner sphere contribution λ_{in} is expected to be smaller with a neutral imidazole ligand than with a negatively charged thiolate. This is supported by theoretical calculations carried out on 2Fe−2S clusters, which show that λ_{in} is decreased by 0.4 eV when two His ligands are substituted for Cys.[29] Moreover, because residue 184 is exposed to the solvent, this substitution should decrease the outer sphere contribution as well. This is because upon reduction of a 4Fe−4S cluster, the added electron is essentially distributed between the bridging sulfurs and the ligands,[30] and the reorganization of the solvent is much weaker when the excess charge is delocalized through the imidazole ring.

Intermolecular Electron Transfer. An interesting result of this work is the evaluation of the rate constant for the intermolecular electron transfer between the distal 4Fe−4S center of a NiFe hydrogenase and its physiological acceptor, cytochrome c_3. Our analysis shows that k_2 is in the range 1050−3500 s^{-1} in the WT enzyme (Figure 6a). Because NMR studies have shown that intramolecular transfers between the four hemes are much faster,[31] k_2 can be identified with the rate constant for the electron transfer from the distal cluster to the closest heme, which is heme 4 according to a NMR study of the complex between the cyt c_3 and the NiFe hydrogenase from *D. vulgaris* Myazaki. In the most probable structure of this complex, the distance between the Fe atom of heme 4 and the closest Fe atom of the distal cluster is equal to 14 Å, and the His ligand is expected to be involved in the electron transfer pathway.[11] Unfortunately, no interval could be obtained for k_2 in forms of the enzyme where His 184 was changed into Gly or Cys, so that the effect of these mutations on the intermolecular transfer cannot be appreciated. However, our previous electrochemical investigation of the H184C and thiol-inhibited H184G forms showed that interfacial (enzyme to electrode) electron transfer is greatly slowed when the distal cluster has an all-sulfur coordination.[16]

We next consider electron transfer to the artificial acceptor methyl viologen. In the WT, P238C, and H184 C forms of the enzyme, this transfer takes place normally via the distal 4Fe−4S cluster. The intermolecular rate constant is decreased 15-fold when His is replaced by Gly (Figure 6a,b), showing that the His ligand of the distal center plays an important role. In the other variants, transfer via the "normal" chain is very slow, and electrons are transferred directly from the medial center to MV. This short circuit takes place when k_{cat} is smaller than about 400 s^{-1} when the medial center is a 4Fe−4S cluster (Figure 6b,c), and smaller than about 25 s^{-1} when the medial center is a 3Fe−4S cluster (Figure 6c). The difference between these numbers can be explained by the fact that ΔE° values for a direct transfer to MV are about −200 mV when the medial center is a 4Fe−4S and −500 mV when it is a 3Fe−4S cluster. This phenomenon questions the use of artificial electron donors or acceptors to study the mechanism of redox enzymes. Whether these mediators interact at the same site of the enzyme as the physiological partner is often unknown. This does not matter as far as one is interested in changes in activity caused by modifications of the enzyme far from this site, like at the active site of the enzyme or in the channel used to transport the substrate,[32,33] but it is of course of great relevance in mechanistic studies devoted to electron transfer chains, as in the present work.

CONCLUSION

Several points emerge from this detailed kinetic study of the electron transfer chain of NiFe hydrogenase. We have first shown that the fact that the turnover number depends on the acceptor does not suffice to demonstrate that the intermolecular step is rate-limiting in the native enzyme (see the above comparison of the WT and P238C forms); this is in contrast to what has been suggested before, including in our own work.[16,34,35] Of course, the conclusion would be different if the change of acceptor led to a variation of k_{cat} greater than an order of magnitude.

Our results also underscore that factors related to details of the protein and to the electronic structure of the FeS clusters play an important role in the efficiency of this chain. This includes the inner sphere and outer sphere contributions to the reorganization energy, the electronic distribution on the redox centers, and details of the electron tunneling pathways. Obviously, simple empirical models in which the λ value is set arbitrarily and the only parameters are the redox potentials and center-to-center distances cannot explain the observed rates and their variations. For example, the Dutton−Moser model[9] predicts $k_4 = 5 \times 10^4$ s^{-1} using the arbitrary value of $\lambda = 0.7$ eV, whereas we found $k_4 > 1500$ s^{-1} in the WT form and $k_4 = 1.5$ s^{-1} in H184C. Detailed calculations of the reorganization energy and of the electronic factor based on the structure of the protein[19] are therefore needed.

Our last comment concerns the kinetic model used to analyze the steady-state activities. A point that is nearly always dismissed when dealing with electron transfer chains is how to deduce the steady-state rate of ET across the entire chain from the values of the individual ET rate constants. When electrons are transferred in a series of irreversible steps, as occurs, for example, in photosynthetic reaction centers, the overall rate is simply obtained by summing the reciprocal of the forward rate constants. This would be wrong in the case of redox enzymes where the electron transfer steps are reversible. The present work therefore adds to the very few studies where the reversibility of the electron transfer steps has been considered.[2,8,36,37]

ASSOCIATED CONTENT

Supporting Information. Steady-state rate equation, potentiometric titration of the FeS clusters of the P238C/H184G variant monitored by EPR, notes about literature values of reorganization energies, and complete ref 33. This material is available free of charge via the Internet at http://pubs.acs.org.

AUTHOR INFORMATION

Corresponding Author
bertrand@ifr88.cnrs-mrs.fr

ACKNOWLEDGMENT

We are grateful to Prof. Hideo Akutsu and Dr. Yuki Takayama for providing us the plasmid pKFC3 used for expression of *Dv*MF cytochrome c3 in *S. oneidensis*.

REFERENCES

(1) Fisher, H. F. *Acc. Chem. Res.* **2005**, *38*, 157–166.
(2) Alric, J.; Lavergne, J.; Rappaport, F.; Vermeglio, A.; Matsuura, K.; Shimada, K.; Nagashima, K. V. *J. Am. Chem. Soc.* **2006**, *128*, 4136–4145.
(3) Pilet, E.; Jasaitis, A.; Liebl, U.; Vos, M. H. *Proc. Natl. Acad. Sci. U.S.A.* **2004**, *101*, 16198–16203.
(4) Tegoni, M.; Silvestrini, M. C.; Guigliarelli, B.; Asso, M.; Brunori, M.; Bertrand, P. *Biochemistry* **1998**, *37*, 12761–12771.
(5) Verkhovskaya, M. L.; Belevich, N.; Euro, L.; Wikstrom, M.; Verkhovsky, M. I. *Proc. Natl. Acad. Sci. U.S.A.* **2008**, *105*, 3763–3767.
(6) Cammack, R.; Frey, M.; Robson, R. *Hydrogen as a Fuel, Learning from Nature*; Taylor and Francis: London and New York, 2001.
(7) Bertrand, P.; Dole, F.; Asso, M.; Guigliarelli, B. *J. Biol. Inorg. Chem.* **2000**, *5*, 682–691.
(8) Leger, C.; Lederer, F.; Guigliarelli, B.; Bertrand, P. *J. Am. Chem. Soc.* **2006**, *128*, 180–187.
(9) Page, C. C.; Moser, C. C.; Chen, X.; Dutton, P. L. *Nature* **1999**, *402*, 47–52.
(10) Rousset, M.; Montet, Y.; Guigliarelli, B.; Forget, N.; Asso, M.; Bertrand, P.; Fontecilla-Camps, J. C.; Hatchikian, E. C. *Proc. Natl. Acad. Sci. U.S.A.* **1998**, *95*, 11625–11630.
(11) Yahata, N.; Saitoh, T.; Takayama, Y.; Ozawa, K.; Ogata, H.; Higuchi, Y.; Akutsu, H. *Biochemistry* **2006**, *45*, 1653–1662.
(12) Matias, P. M.; Soares, C. M.; Saraiva, L. M.; Coelho, R.; Morais, J.; Le Gall, J.; Carrondo, M. A. *J. Biol. Inorg. Chem.* **2001**, *6*, 63–81.
(13) Peters, J. W.; Lanzilotta, W. N.; Lemon, B. J.; Seefeldt, L. C. *Science* **1998**, *282*, 1853–1858.
(14) Jormakka, M.; Richardson, D.; Byrne, B.; Iwata, S. *Structure* **2004**, *12*, 95–104.
(15) Sazanov, L. A.; Hinchliffe, P. *Science* **2006**, *311*, 1430–1436.
(16) Dementin, S.; Belle, V.; Bertrand, P.; Guigliarelli, B.; Adryanczyk-Perrier, G.; De Lacey, A. L.; Fernandez, V. M.; Rousset, M.; Léger, C. *J. Am. Chem. Soc.* **2006**, *128*, 5209–5218.
(17) Teixeira, M.; Moura, I.; Xavier, A. V.; Huynh, B. H.; DerVartanian, D. V.; Peck, H. D., Jr.; LeGall, J.; Moura, J. J. *J. Biol. Chem.* **1985**, *260*, 8942–8950.
(18) Fernandez, V. M.; Hatchikian, E. C.; Patil, D. S.; Cammack, R. *Biochim. Biophys. Acta* **1986**, *883*, 145–154.
(19) Hayashi, T.; Stuchebrukhov, A. A. *Proc. Natl. Acad. Sci. U.S.A.* **2010**, *107*, 19157–19162.
(20) Leroux, F.; Dementin, S.; Burlat, B.; Cournac, L.; Volbeda, A.; Champ, S.; Martin, L.; Guigliarelli, B.; Bertrand, P.; Fontecilla-Camps, J.; Rousset, M.; Léger, C. *Proc. Natl. Acad. Sci. U.S.A.* **2008**, *105*, 11188–11193.
(21) Ozawa, K.; Tsapin, A. I.; Nealson, K. H.; Cusanovich, M. A.; Akutsu, H. *Appl. Environ. Microbiol.* **2000**, *66*, 4168–4171.
(22) Ozawa, K.; Takayama, Y.; Yasukawa, F.; Ohmura, T.; Cusanovich, M. A.; Tomimoto, Y.; Ogata, H.; Higuchi, Y.; Akutsu, H. *Biophys. J.* **2003**, *85*, 3367–3374.
(23) Ozawa, K.; Yasukawa, F.; Fujiwara, Y.; Akutsu, H. *Biosci. Biotechnol. Biochem.* **2001**, *65*, 185–189.
(24) Voordouw, G.; Pollock, W. B.; Bruschi, M.; Guerlesquin, F.; Rapp-Giles, B. J.; Wall, J. D. *J. Bacteriol.* **1990**, *172*, 6122–6126.
(25) Leger, C.; Bertrand, P. *Chem. Rev.* **2008**, *108*, 2379–2438.
(26) Léger, C.; Dementin, S.; Bertrand, P.; Rousset, M.; Guigliarelli, B. *J. Am. Chem. Soc.* **2004**, *126*, 12162–12172.
(27) Benosman, H.; Asso, M.; Bertrand, P.; Yagi, T.; Gayda, J. P. *Eur. J. Biochem.* **1989**, *182*, 51–55.
(28) Volbeda, A.; Charon, M. H.; Piras, C.; Hatchikian, E. C.; Frey, M.; Fontecilla-Camps, J. C. *Nature* **1995**, *373*, 580–587.
(29) Sigfridsson, E.; Olsson, M. H.; Ryde, U. *Inorg. Chem.* **2001**, *40*, 2509–2519.
(30) Noodleman, L.; Lovell, T.; Liu, T.; Himo, F.; Torres, R. A. *Curr. Opin. Chem. Biol.* **2002**, *6*, 259–273.
(31) Louro, R. O. *J. Biol. Inorg. Chem.* **2007**, *12*, 1–10.
(32) Dementin, S.; Burlat, B.; De Lacey, A. L.; Pardo, A.; Adryanczyk-Perrier, G.; Guigliarelli, B.; Fernandez, V. M.; Rousset, M. *J. Biol. Chem.* **2004**, *279*, 10508–10513.
(33) Liebgott, P. P.; et al. *Nat. Chem. Biol.* **2010**, *6*, 63–70.
(34) Pershad, H. R.; Duff, J. L.; Heering, H. A.; Duin, E. C.; Albracht, S. P.; Armstrong, F. A. *Biochemistry* **1999**, *38*, 8992–8999.

(35) De Lacey, A. L.; Santamaria, E.; Hatchikian, E. C.; Fernandez, V. M. *Biochim. Biophys. Acta* **2000**, *1481*, 371–380.
(36) Santabarbara, S.; Heathcote, P.; Evans, M. C. *Biochim. Biophys. Acta* **2005**, *1708*, 283–310.
(37) Bertrand, P.; Asso, M.; Mbarki, O.; Camensuli, P.; More, C.; Guigliarelli, B. *Biochimie* **1994**, *76*, 524–536.